Mechanical characterization of 3D-printed components

Catarina Simão Correia
catarina.correia@tecnico.ulisboa.pt

Instituto Superior Técnico, Universidade de Lisboa, Lisboa, Portugal

November 2019

Abstract

Although additive manufacturing is a recent subject, it is of great interest and consequently much investigation. Nevertheless, the variety of processes, parameters and applications makes the possibilities of construction almost infinite, becoming hard to accomplish a full knowledge. In order to contribute to that knowledge, this work intends to characterize the mechanical behaviour of PLA structures printed with FDM technology, in particular the elasto-plastic transition, taking into account the infill density and the raster orientation. With that objective, quasi-static and cyclic tests were conducted, each one of them under two types of uniaxial loading: tensile and compressive. The densities and the volumes of the compressive specimens were experimentally measured by the Archimedes method, allowing to compare the values obtained with a reference density and to determine the variation of volume that occurred during the compression test. It was possible to identify different deformation phases on the curves obtained and draw some conclusions on the influence that the two parameters under investigation have on the mechanical behaviour of the structure.

Keywords: Additive manufacturing, mechanical characterization, PLA, density, deposition angle

1. Introduction

Additive manufacturing consists on building parts by progressively adding material, instead of removing it from an initial block as in subtractive manufacturing. This kind of fabrication allows a huge flexibility in design since the parts are built from a computational model, which can even enable the manufacturing of parts that would be difficult to produce by other means[1]. That also allows to reduce the wastage which, with some expensive materials, can mean a save in costs. Additive manufacturing is also advantageous compared with other processes in cases where it is aimed to build prototypes, personalized objects or small batches since it doesn't have the need of developing and producing moulds. The variety of processes included in this kind of fabrication enables the production of parts on a wide range of sizes and materials. The precision and surface finish of the parts depend on the method selected and can also be influenced by its parameters [2].

The parts produced by means of additive manufacturing may find application in various and significant industries, such as the automotive, aerospace and biomedical [2]. For example, in the case of the aerospace and aeronautics industries, the possibility of producing complex geometries (such as the honeycomb cell) means that additive manufacturing gives a strong contribute for the accomplishment of one of their biggest objectives: obtaining weight to resistance ratios increasingly small [1].

The first form of additive manufacturing, named Stereolithography, emerged in the 80's. At the beginning, the main objective was the fabrication of small models and prototypes. However, the investigation and development of this subject have been changing the focus of additive manufacturing, making it also able to cover the production of small parts for final use on their applications[1, 2]. This makes of great importance to know deeply the process that is intended to be used and its variables, in order to predict, to a certain level, the final characteristics and mechanical properties of the obtained part.

1.1. FDM: process and parameters

There is a wide range of processes of additive manufacturing that differ from one another, for instance, on the materials they use and the dimensions of parts they are recommended to build. Some examples of these methods include the Stereolithography, the Powder Bed Fusion processes, the Direct Energy Deposition and the Fused Deposition Modeling.

This last process, patented in 1989 by *Stratasys*, also known as Fused Filament Fabrication is of widespread use, being the process commonly existent on the desktop 3D printers.

The basics of this process include the fusion of a thermoplastic filament that is progressively deposited on a platform. As in the other methods of additive manufacturing, the process begins with the computational model of the part to be produced. Then it is necessary to send the file obtained to a slicer software, that is, a software whose function is to stablish the parameters that will allow to build the part layer by layer. When all the parameters have

been defined, the software generates a g-code that is transmitted to the printer.
The printers are usually composed of a print head and a platform where the part is constructed. After each layer is completed, the print head and the platform increase their distance by an amount correspondent to the layer height.
The printing parameters can influence not only the mechanical properties, but also the surface finish of the manufactured parts. Some of the commonly adjusted parameters include, among many others, the building direction, the deposition angle, the infill density and the layer's height.
The building direction can be defined as the direction whereby the layers are progressively deposited. Changing this parameter can have influence on the strength and the type of fracture of the printed structures. The bonding between layers is weaker than the filament itself. That means that, if the building direction leads to layers perpendicular to the direction of applied load, the consequence will be a reduced resistance [3,4]. The building direction also has direct influence on the necessity of using support material.
The angle formed between the direction of the deposited filament and a reference direction is called the deposition angle (figure 1). This parameter can have an influence similar to that of the building direction.[5 ,6].

Figure 1: Deposition angle: 90º (left), 0º (middle) and 45º (right) [6]

The investigation of the influence of the layer's height has produced conflicting results. Some studies affirm that reducing this parameter results in an upgrade of the strength [7, 8]; others affirm that, for the same nozzle diameter, reducing the layer height leads to smaller porosities and, consequently, to an increase of the resistance [7, 9]. The layer height also impacts on surface finish, on dimensional errors and in the building time: the higher the layer height, the less the layers needed to build a part and the less the time needed for construction [3, 4].
There are also another kind of exterior parameters that can influence the final properties of the parts, like the colour of the filament [7, 10] and the absorption of moisture [11]

1.2. Polymers

Polymers are formed by atoms that repeat themselves (monomers) along a polymer chain [12]. These materials can be grouped based on their molecular structure and consequent behaviour.
Thermoplastics are polymers which monomers are tangled, without forming strong links. When heated, these polymers behave like viscous liquids, which means they can be moulded [13]. If the polymer chains form strong links, it constitutes a thermoset. After being solidified, these polymers don't return to the liquid state, which means the heat will only degrade them, not allowing them to be moulded [13].
In contrast to metals, where the internal structures are extremely organized (crystalline structures), polymers form disorganised and tangled structures, named amorphous structures. Amorphous polymers can be manipulated in order to organize to their structure. In cases where some organised regions (crystalline regions) coexist with amorphous structures, the polymer is named semi-crystalline [12, 13].
The mechanical characterization of polymers aims not only to observe their macroscopic behaviour, but also try to relate this behaviour with its molecular structure [12, 14].
The mechanical behaviour of polymers is highly influenced by the testing conditions, making it difficult to classify them [12, 13, 15]. The glass transition temperature points out the beginning of the softening of the polymer, that is, the moment when the polymer begins to present viscous characteristics instead of fragile solid behaviour [12, 13].
The mechanical behaviour is said to be elastic when there exists a reversible relation between applied load and resultant deformation, that is, the material recovers its original shape when the load is removed. On viscous behaviour, the deformations remain even after the load has been removed. When the material presents simultaneously elastic and viscous characteristics, it is said to be viscoelastic. One of the main features of this kind of behaviour is its high dependence on time [14].
The behaviour of glassy polymers has been deeply investigated. Typically, beyond the yield point, two trends are observable: a yield drop immediately after the yield point, i.e., the stress tends to decrease with increasing deformation and, at large deformations, strain hardening, i.e., the stress increases with increasing deformation. This drop has been seen as an intrinsic material softening, although there's still no unanimously accepted explanation. Some studies affirm that this softening may influence the initiation of strain localization [15], some others affirm that its amplitude is depends on the competition between two phenomena, the polymer aging and rejuvenation.

1.3. PLA

Polylatic Acid (PLA) is a thermoplastic derived from lactic acid. Its biocompatibility makes its use on medical applications a subject of great interest and hence great investigation in order to understand the origin of the failures that occur and, if possible, avoid

them. Some studies reveal that PLA shows some characteristics of the glassy polymers, for example, it shows strain softening after the yield point, followed by strain hardening [16]. Additionally, its behaviour also shows a high dependence on time and on the strain rate [16, 17].
PLA is one of the most commonly used materials on FDM printers. Its glass transition temperature and its melt temperature round 60ºC and 145ºC-160ºC, respectively [18]. The relatively low glass transition temperature is, at the same time, an advantage, because it requires less energy to be processed, and a disadvantage, because it diminishes its performance at high temperatures [7, 18]. Relatively to ABS (another of the most commonly used polymers in FDM), PLA shows a lower thermal expansion coefficient (which results in parts with less warping), and greater elasticity modulus and strength. It is also advantageous with respect to the particle emission during printing, despite due to its biodegradation, shows a shorter durability.

2. Methods

The experimental work included uniaxial tensile and compression quasi-static tests and uniaxial tensile and compression cyclic tests. Two process parameters were selected in order to assess its influence on the mechanical behaviour of printed structures: infill density and deposition angle. Three levels of variation were evaluated for each of them, 50%, 75% and 100% for the infill density, and 0º, 90º and ±45º for the deposition angle.
For each combination of those parameters, nine tensile specimens and nine compression specimens were printed, in a total of 81 tensile and 81 compression specimens. The specimens were printed with an *Ultimaker 3 Extended* and the remaining printing parameters available on Cura software were kept constant in all the prints. All the specimens were printed with one exterior wall, formed by a single contour, and the specimens with infill percentages lower than 100% were printed with two layers at the bottom and two layers at the top completely dense. The deposition angles aforementioned referred to the load direction of the mechanical tests, as illustrated on figure 2.

Figure 2: Schematics of the applied load

The beginning point of each layer becomes salient and because of that it was imposed to be random, attempting to minimize the existence of vertical lines composed of these points. Printing the specimens directly on the glass plate gives them a mirrored finish.
Preliminary tests of this work revealed that this feature conditioned the deformation of the specimens, contributing for its inhomogeneity. Due to this fact, it was decided to print all the specimens on a printed base, attempting to approximate the finishing of all faces of the specimens. The specimens were removed from this base (named *raft* on Cura) after the printing.
The mechanical tests were performed on a universal testing machine Instron 5966 with a load cell of 10 kN (figure 3). To alternate between the different types of tests possible to perform on this machine it is necessary to change its accessories. In this work compression plates and tensile grips were used.

Figure 3: Instron 5966 – universal testing machine

The testing machine transmits the load and the displacement during each test to a computer and allows to use strain extensometers.
The communication between the testing machine and the computer is assured by a specific software, the *Bluehill*. In this software it is possible to define the test parameters. It also allows to choose which experimental data acquired during the test should be recorded and exported to a file.

2.2. Measurements

After being printed, all the compression specimens were weighted on a precision balance *Mettler Toledo ML204* (figure 4). The use of the density kit (*Density Kit ML-DNY-43*) enabled the determination of each specimens' density before and after the mechanical test by applying the Archimedes principle. The results from this determination made possible the evaluation of the real infill percentages of the specimens, as well as of the volume variation occurred during the uniaxial compression tests. For the application of the principle, the specimen should be firstly weighted on air and, after that, on a liquid with known density.
Beside the compression specimens, two excerpts of filament were also weighted: one of them taken

directly from the spool and the other after being extruded. Due to the reduced dimensions of the extruded filament, a group of filaments had been used instead of just an individual filament.
The experimental volume of each specimen allowed to determine its cross section, after measuring the correspondent height with a caliper.

Figure 4: Precision scale - Mettler Toledo ML204

2.3. Uniaxial compression test

At this point, there are still no specific standards for mechanical testing of parts produced by additive manufacturing. Therefore, for the mechanical tests of this work the standards concerning the mechanical tests of plastics have been taken as reference. For the uniaxial compression tests, the ASTM D 695 standard was adopted.
Preliminary tests of this work revealed that the force needed to compress the specimens with the geometry recommended on the standard exceeded the load capacity of the testing machine. Because of this, it was decided to modify the geometry, keeping the parallelepiped shape with a quadrangular base with 10 mm side and a height of 15 mm in order to try to assure a uniform deformation of the specimens during the test, which was performed with a constant speed, v=1,3 mm/s. For each combination of infill density and deposition angle, five specimens were tested and, in order to reduce the friction, teflon tape was applied between the specimen and the compression plates.
During each test, the values of force and displacement of the upper compression plate were recorded to obtain the force-displacement curve and to determine the engineering values of stress and strain, according to what is recommend by the standard. The evaluated properties were also the ones indicated as of interest by the standard, i.e., the yield stress and strain and the modulus of elasticity.
On compression tests, the curves may show a non-linear beginning, which is not a true response of the material but rather an adaptation of the specimen geometry or alignment to the compression plates. In those cases, the standard indicates the procedure to correct the beginning of the experimental curve.

2.4. Uniaxial tensile test

Again, these tests followed the standards concerning the mechanical tests of plastics, in this case, the ASTM D 638 was adopted, and the type I specimens were selected. For each combination of infill density and deposition angle five specimens were tested. The same testing machine was used for these tests, but this time two extensometers (transversal and longitudinal) were used (figure 5). The tests were performed up to the occurrence of fracture of the specimens. The properties evaluated were those referred on the standard, i.e., the yield stress and strain, the fracture stress and strain, the modulus of elasticity and the Poisson's coefficient.

Figure 5: Extensometers in uniaxial tensile test

2.5. Cyclic tests

Beside the quasi-static tests, uniaxial and compression cyclic tests were also performed, with two specimens tested for each combination of infill density and deposition angle, in a total of 18 tensile specimens and 18 compression specimens. In this kind of test it is necessary to define the loading and unloading conditions for each cycle, which limits can be defined in terms of force/stress applied or displacement/strain imposed. In this work, the limits were defined considering the mechanical behaviour observed, for each specimen, on the quasi-static tests.

3. Results and discussion

3.1. Densities and dimensions

The determination of the density of the filament before and after testing led to the conclusion that before the extrusion the filament had a density slightly higher than the theoretical density indicated by the technical sheet of the filament manufacturer and that after the extrusion this density becomes slightly lower than the theoretical. However, due to its small dimensions, the measurement of the density of the extruded filament was difficult, resulting in dispersed results. Therefore, in order to determine the relative density of the specimens with infill densities lower than 100%, the mean value of the

densities of the specimens with 100% for each deposition angle was taken as reference (table 1).

Table 1 Relative densities

Relative densities [g/cm³]			
	0º	90º	±45º
Density (reference)	1,236	1,240	1,238
100%	1	1	1
75%	0,760	0,757	0,750
50%	0,549	0,568	0,580

These results allow to conclude that the density of the specimens with infill of 75% approximately match 75% of the value taken as reference and the density of the specimens with infill of 50% is slightly higher than 50% of the reference value.

The specimens' dimensions were determined before the tests. In the case of the tensile specimens, the dimensions of the cross section were measured using callipers. In the case of the compression specimens, the measurements of the height with a calliper were affected by irregularities of the surface and by the differences of the geometry in relation to the parallelepiped geometry defined on project. Then, it was decided to measure the cross section of compression specimens (since those lateral faces were more regular) and calculate the height based on this value and the measured volume.

3.2. 100% infill specimens

The determination of the volumes before and after the mechanical test permitted to analyse the volume variation of the compression specimens. These results showed that, in the case of specimens with 100% infill, the variation was not significant and then enabled the determination of the true stress and true strain values. Naturally, the variation in the case of the specimens with infill densities lower than 100% were much more significant.

Due to the limitations of space on the balance, the analyses of the volumes were only made on the compression specimens. Nevertheless, the results were considered to be true also in the case of the tensile specimens and the true stress-strain curves were also obtained to this case.

3.2.1. Uniaxial tensile test

Figures 6 and 7 represent the engineering stress-strain curves and true stress-strain, respectively.

The observation of these figures allows to conclude not only that the curves of each deposition angle have a high repeatability, but also that the engineering and the true stress-strain curves are identical.

The analysis of these curves allows to distinguish various regions. Firstly, it can be immediately identified a point of maximum stress, preceded by linear region. A more detailed examination reveals

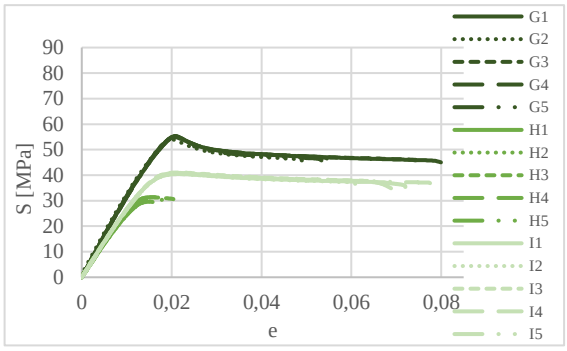

Figure 6: Engineering stress-strain curves from tensile tests of specimens with 100% infill

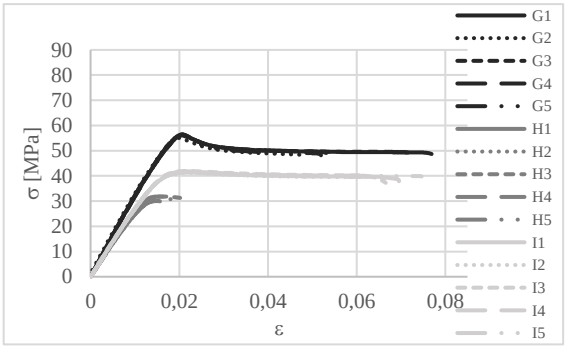

Figure 7: True stress-strain curves from tensile specimens with 100% infill

that the region before the maximum stress is not completely linear, being the site where this non-linear region starts coincident to the end of the region where the behaviour is only elastic.

The cyclic tests performed in this work aimed to improve the comprehension of this non-linear zone and quantify, at the end of each cycle, an elastic component of the deformation, corresponding to the strain that is recovered on the unloading path, and another part, here named inelastic, that corresponds to the difference between the total strain imposed at the end of the cycle, and the elastic component. Representing the points of maximum stress of each cycle it can be concluded that the cycles do not influence significantly the shape of the curve (figure 8).

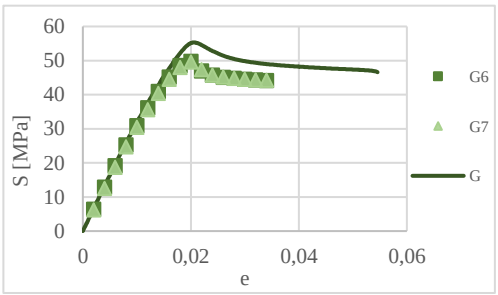

Figure 8: Maximum points of the cyclic test and quasi-static curve of specimens with 100% infill and deposition angle of 0º

From the examination of the complete cyclic curves obtained, it is possible to detect that the slope of the loads and unloads change between cycles. On an attempt to account for this variation, the slope from

an initial cycle was taken as reference, that is, it was assumed as representative of a purely elastic unload. Consequently, straight lines with that slope were plotted at the end of each cycle, representing what would be the respective unload if it was purely elastic. The difference between the elastic component of strain previously identified and this new "purely elastic" strain component was assumed to be a viscoelastic part. It was also assumed that the point where this viscoelastic strain becomes significant should match approximately the beginning of the non-linear region. Therefore, the evolutions of these strain components allowed to identify, approximately, the transition from linear region to non-linear region in the stress-strain curves for each type of specimen. An example of this analysis is shown in figure 9, where "e_I" represents the inelastic strain, "e_E" the elastic strain and "e_{EP}" the purely elastic strain. These evolutions also confirm that the elastic component tends to stabilize approximately at the instant corresponding to the defined yield point, which in polymers is defined as the point where an increase in deformation occurs without a correspondent increase in stress.

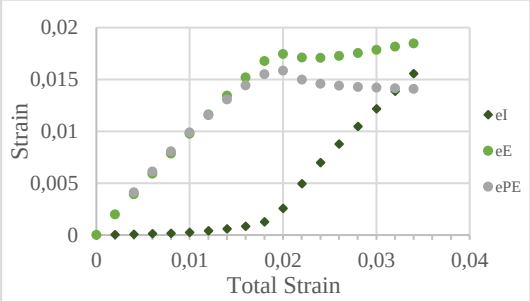

Figure 9: Evolution of the strain components in the tensile test of a specimen with 100% infill and deposition angle of 0º

The mechanical behaviour is assumed to result from the contribution of various factors, for example, the material, the testing conditions and the geometry. When it concerns to geometry, the dimensional variation during test can contribute to promote the deformation or to make it more complicated. In order to quantify this influence, it was again considered that the volume remained constant during deformation and, with this assumption, the cross-section area of each specimen was determined at each instant along the experimental tests. Then, considering a constant stress, it was possible to determine the force that would be necessary to continue the deformation after the first maximum point if this force was only dependent on the variation of the area. This analysis was made for three tensile specimens, one of each deposition angle. Figure 10 represents the result of this analysis in the uniaxial tensile test of a specimen with 100% infill and a deposition angle of 0º, where the continuous line represents the recorded force during the test and the dashed line represents the force determined following the above mentioned conditions.

As expected, the force due to variation of cross-section area decreases during the tensile test as the cross-section area is reduced during the test. Nevertheless, at some instants the experimental force decays more than that determined force. This shows that there are other phenomena influencing the deformation.

The biggest decay after the maximum point is verified on the specimens with deposition angle of 0º. This yield drop, known as "strain softening" can be associated to some phenomena on the interior of the polymers, though there's still no accepted justification, as mentioned before. One possible justification is that this drop can be associated to the emergence of small localized regions where the deformation is more intense. The observation of figure 10 also shows that, at a certain moment, the force recorded and the calculated force begin to show the same slope. Therefore, it is assumed that the maximum point corresponds to the emergence of regions with localized deformation that later propagate, originating a deformation approximately uniform and causing a decrease in force equivalent to the decrease caused by the reduction of the area, suggesting that this becomes the only cause of the variation of the force.

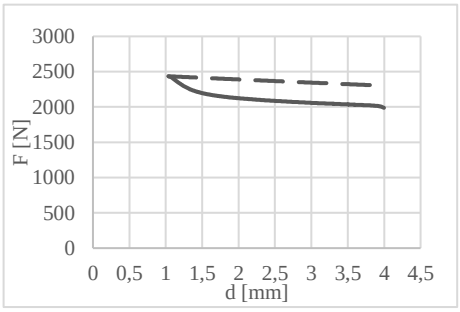

Figure 10: Force recorded (continuous line) and calculated force (dashed line); tensile specimen with 100% infill and deposition angle of 0º

The same analysis was made to the remainder 100% infill specimens. The specimens with deposition angles of 90º and ±45º also show a linear and a non-linear region before the maximum point. However, the specimens with deposition angles of 90º do not show a significant yield drop. An observation of the fracture surface of the specimens led to the conclusion that the fracture of the 90º specimens is fragile, taking place between adjacent filaments, while the other fractures are ductile and occur within the filament itself. The behaviour of the stress-strain curves of the specimens with deposition angles of ±45º look like an intermediate of the previous two cases. These specimens can sustain deformation levels like those of the specimens of 0º, however, the behaviour of their curves differ immediately after the maximum point. The force recorded in the case of the specimens with deposition angles of ±45º seems to follow the force determined due to the variation of the area since the maximum point. This may be consequence of the internal structure. Since the

filaments are in ±45º, the vertical applied load is divided into a component aligned with the filament and another perpendicular to that. This could mean that the stress in each filament is slightly lower, sufficient to deform uniformly the specimen, but insufficient to originate zones of localized deformation.

3.2.2. Uniaxial compression test

The compression tests' experimental data were analysed in a similar way as the results from the tensile test were. Accordingly, the figures 11 and 12 represent the experimental engineering and the true stress-strain curves, respectively.

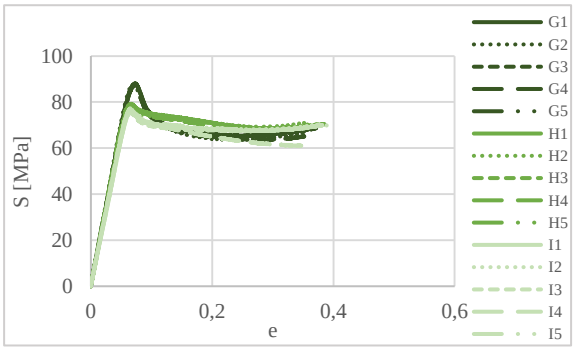

Figure 11: Engineering stress-strain curves from compression tests of specimens with 100% infill

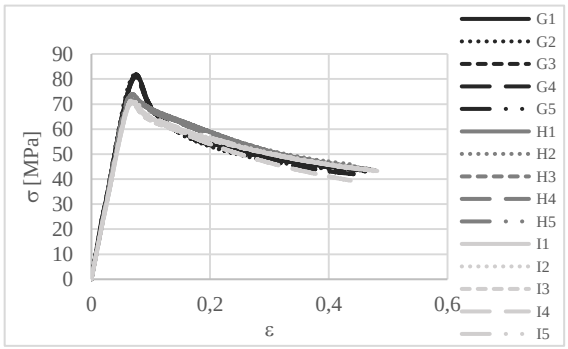

Figure 12: True stress-strain curves from compression tests of specimens with 100% infill

In contrast to what was verified in the case of the tensile curves, in this case the engineering and the true stress-strain curves are significantly different. The true stress-strain curves show a continuously decreasing behaviour, whereas the engineering stress-strain curve show, from a certain moment, an increasing behaviour. However, taking into account the levels of deformation imposed to the compression specimens and the conditions observed during the mechanical test, it can be concluded that the behaviour of this true stress-strain curve is not exclusively representative of the material, being possibly influenced by the instability of the deformation, that cease to be uniform way before the end of the test. Despite this, the engineering and the true stress-strain curves show similar behaviours until the maximum point.

Since the curves obtained from the uniaxial compression tests exhibit a non-linear region in the beginning of the test (as a result of the adaptation), it is not possible to ensure that the slope of the first cycles of the cyclic test are not already influenced by this adaptation and plastic deformation localized at the tops of the specimens (due to their irregular geometry). Because of this, the analysis made before to determine where the linear region ends was not carried out for the case of compression tests. However, it is still possible to note that, again, the cycles do not affect significantly the behaviour of the stress-strain curve (figure 13)

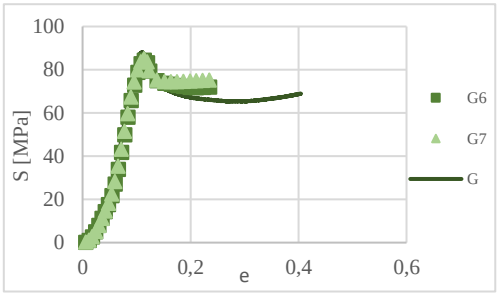

Figure 13: Maximum points of the cyclic test and quasi-static curve of specimens with 100% infill and deposition angle of 0º

As before, the effect of the variation of the section area was quantified, using the same strategy. Again, this analysis was made for three compression specimens, with figure 14 representing one of them.

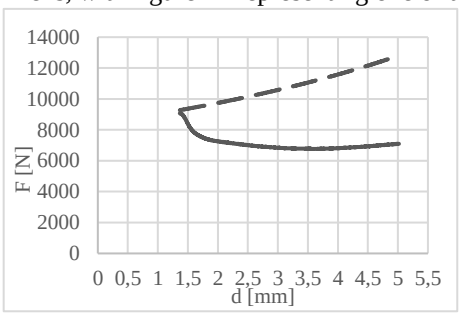

Figure 14: Force recorded (continuous line) and calculated force (dashed line); compression specimen with 100% infill and deposition angle of 0º

The influence of the area is again coincident to what was expected: in this case, the area is increasing during the test, causing an increase of the necessary force. Also, as before, the force recorded differs from the force calculated. This time, even their behaviour is different. It is then assumed that the decreasing behaviour of the recorded force curve, verified in all the deposition angles, is a consequence of the instability of the deformation, mentioned before. The deformation concentrates in some regions of the specimen, enabling the global deformation of the structure. When this deformation reaches a limit, it tends to try to propagate to the rest of the specimen, causing an increase in force. The justification for the biggest decay verified on the

specimens with deposition angle of 0º is similar to that presented for the tensile results.

3.2.3. Tensile versus compression

Comparing the results for both cases, some conclusions can be taken. Regardless of the deposition angle considered, the shape of the curves until the maximum point is similar. It is also verified that, for both cases, the specimens with deposition angle of 0º show higher strength and the biggest decay after the yield point, compared with the other directions.

It can also be concluded that the maximum tensile stress (the yield stress) to deform the specimens is lower than the maximum compressive stress, while the modulus of elasticity is higher in the case of the tensile test than in the compressive test.

3.3. Other infill densities

3.3.1. Uniaxial tensile test

As referred before, the true stress-strain values only can be determined in the cases of 100% infill density, so, in the figures 15 and 16 there are represented the engineering stress-strain curves of the 75% and 50% infill densities.

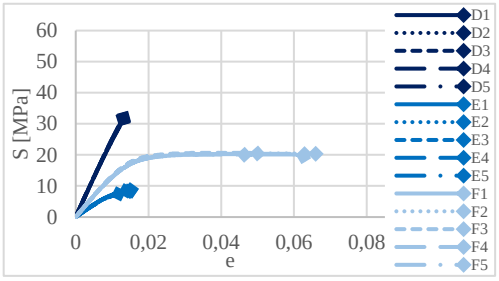

Figure 15: Engineering stress-strain curves from tensile tests of specimens with 75% infill

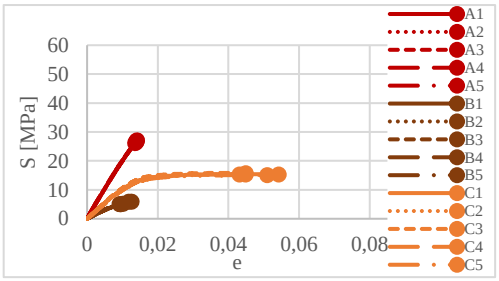

Figure 16: Engineering stress-strain curves from tensile tests of specimens with 50% infill

A preliminary analysis allows to conclude that, once again, the repeatability between curves correspondent to the same deposition angle is high. For the deposition angle, the behaviour of the curves between different infill densities is similar, except for the case of 0º, where the behaviour changes from ductile in the case of 100% infill to fragile in the remaining percentages.

One of the most obvious differences relatively to the 100% infill specimens is the decrease of the mechanical strength. This fact is easily explained, since lower densities imply less material available in the interior of the specimen to sustain the deformation.

The engineering values were determined using the values of the force and displacement recorded and the exterior dimensions of each specimen. However, when the infill is lower than 100%, there will exist empty spaces in the interior of specimens, which means that the exterior area does not correspond to the real resistant area. This real resistant area, resulting from the sum of each filament available to resist, is smaller than the area used on the determination of the engineering stress, which means that the stress actually applied on the filaments on the interior of these structures is greater than the calculated. This way, the curves showed should be interpreted as representative of the totality of the structure, considering the level of porosity.

It can also be noted that the engineering stress-strain curves continue to exhibit a linear and a non-linear region before the maximum point, being the curvature of the non-linear region more marked in the case of specimens with infill densities lower than 100%.

The analysis of the main mechanical properties obtained in the experimental tests allows to conclude that, in general, the specimens with a deposition angle of 0º present higher values for the properties evaluated than the remaining directions, except for the strain on the point of maximum stress and the Poisson coefficient. This difference in the yield strains may be justified by the instant where the fracture occured: in the case of specimens with depositions angles of 0º and 90, the specimens broke just before the maximum stress; the specimens with deposition angle of ±45º reached deformation levels similar to those of specimens with deposition angle of 0º and infill of 100%.

3.2.2. Uniaxial compression test

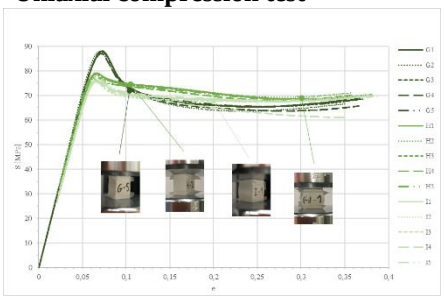

Figure 17: Engineering stress-strain curves from compression tests of specimens with 100% infill

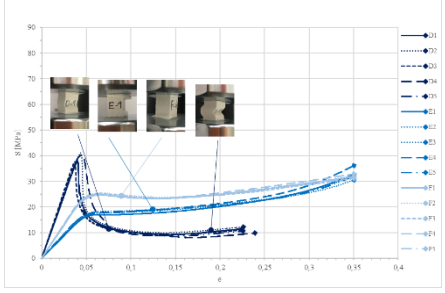

Figure 18: Engineering stress-strain curves from compression tests of specimens with 75% infill

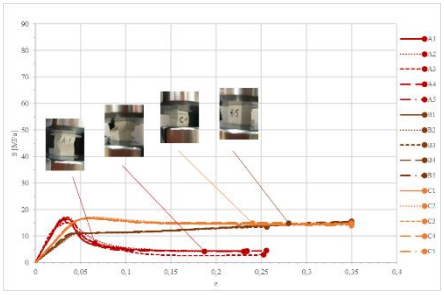

Figure 19: Engineering stress-strain curves from compression tests of specimens with 50% infill

The figures 17 and 18 show the engineering stress-strain curves obtained for the compression specimens with 50% and 75% infill density. The figure 19 shows again the engineering stress-strain curve for the specimens with 100%, with some photos illustrating the specimen's deformation at some instants during the compression tests. During these tests, the specimens reached non-uniform deformation modes, due to instability and layers' separation, just after the maximum of the curves.

The curves of the figures 17, 18 and 19 show the expectable trend of improved mechanical strength with the increase of infill density. Most of the curves exhibit the same kind of decay (strain softening) analysed before and it can be noted that this drop is bigger again in the specimens with deposition angle of 0º. Some curves do not present a local maximum, making it difficult to compare them with the rest of the compression curves.

Once again, the properties evaluated are referring to the mechanical behaviour of the structure and not only dependent of the material.

With the objective of evaluating the real state of solicitation of the material and compare it to the results of the specimens with 100% infill, it was determined a "corrected area" for the calculation of new engineering values. In the printing phase of the specimens, it was chosen to use one exterior contour on each layer, forming something like a frame around the infill. The calculation of the corrected area was done taking into account not only the percentage of area corresponding to the infill conditions, but also considering the area associated with this frame. Knowing that the width of each contour is 0,4 mm, the area corresponding to the frame of each specimen was determined by:

$$A_{frame} = (l_1 \times l_2) - \big((l_1 - 0{,}8) \times (l_2 - 0{,}8)\big)\ mm^2$$

Where l_1 and l_2 are the dimensions of each side of the cross section. Knowing that the area corresponding to the infill is given by the difference between the total area and the area of the frame, $A_{interior\_c} = A_T - A_{frame}\ mm^2$, the resistant area can be determined by:

$$A_{resistant} = A_{frame} + \%_{infill} \times A_{interior}$$

After determining the areas of the resistant cross-section of each compression specimen, the values of engineering stress of the compressive tests were corrected. Figure 20 represents the corrected curves of the specimens with 50% and 75%.

The correction applied to the area results in an increase of the stress values, as would be expected. This increase is more significant with lower densities. However, this increase is not enough to approximate these values of stress to the values obtained with specimens with 100%. This fact can be due to the deformation mode of each geometry, since each specimen with densities lower than 100% contains empty spaces on its interior that enable deformation modes different from those of the specimens with 100% infill.

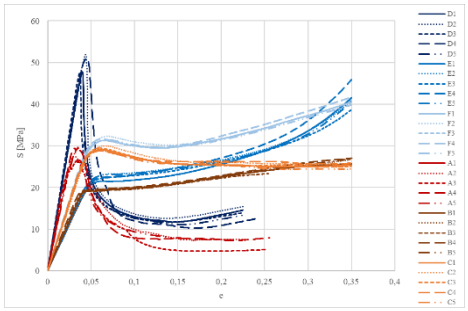

Figure 20: Engineering compression stress-strain curve with corrected values

4. Conclusion

This experimental work intended to analyse the mechanical behaviour of structures fabricated with FDM process. This manufacturing process involves a large variety of printing parameters. From these, two were selected in order to assess its influence: the infill percentage (100%, 75% and 50%) and the deposition angle (0º, 90º, ±45º). It was established that structures fabricated with the combinations of these parameters would be tested in uniaxial tensile and compression loadings with quasi-static and cyclic tests. The quasi-static tests were based on the standard ASTM D 638 (tensile) and ASTM D 695 (compressive). The dimensions of the compression specimens had to be adapted due to load capacity limitations of the testing machine. All the specimens (tensile and compression) were printed with one exterior contour and, in the case of specimens with infill density lower than 100%, with two bottom and two top layers completely dense.

Before the mechanical tests, the dimensions and the densities of all specimens were determined. From the results of the density measurements, it was possible to conclude that the density of specimens with 75% infill density match, approximately, 75% of the density of reference; in the case of specimens with 50% infill, the density was slightly higher (≈55%) than 50% of the reference density. The analysis of the compression specimens volumes before and after the testing allowed to conclude that, in the case of specimens with 100% infill, the variation was of little magnitude. This assumption enabled the

determination of the true stress and strain values, assuming an uniform deformation.

The curves obtained were similar to those typical of polymers, making it possible to identify different phases of the deformation. In particular, the cyclic tests helped with the identification of the viscoelastic component of deformation and, consequently, the identification of the point of transition between the linear and non-linear regions before the maximum point, for the tensile specimens. It was also detected the occurrence of strain softening after the yield point. The influence of the cross section variation on the necessary force was evaluated, leading to the conclusion that this influence, as well as the intrinsic softening of the material, were dependent on the deposition angle. The specimens with the deposition angle of 0º revealed to be the ones with higher mechanical strength and a higher yield drop. In contrast to what was verified on the tensile stress-strain curves, the engineering stress-strain curves obtained from compression tests were significantly different from the true ones. However, it was assumed that these true curves could be influenced by the instability of deformation observed on compression specimens, not being exclusively representative of the material. The evolution of the engineering and true stress-strain curves was similar until the maximum stress.

The results obtained from specimens with infill densities lower than 100% are representative of the entire structures and not the material, since these specimens contain empty spaces on their interior. In the compression tests, a correction of the resistant cross-section area of the specimens was attempted. The engineering values calculated with the determined effective cross-sectional area increased, however, were still much lower than the engineering values obtained for the specimens with 100% infill.

5. Acknowledgements

The author truly acknowledges the MIT-Portugal project “MIT-EXPL/ISF/0084/2017”, funded by Massachusetts Institute of Technology (USA) and “Ministério da Ciência, Tecnologia e Ensino Superior - Fundação para a Ciência e a Tecnologia” (Portugal)

5. References

[1] Wong, Kaufui V., and Aldo Hernandez. "A review of additive manufacturing." ISRN Mechanical Engineering 2012 (2012).

[2] Tuan D., et al. "Additive manufacturing (3D printing): A review of materials, methods, applications and challenges." Composites Part B: Engineering 143 (2018): 172-196.

[3] Qattawi, Ala, Buraaq Alrawi, and Arturo Guzman. "Experimental optimization of fused deposition modelling processing parameters: a design-for-manufacturing approach." Procedia Manufacturing 10 (2017): 791-803.

[4] Chacón, J. M., et al. "Additive manufacturing of PLA structures using fused deposition modelling: Effect of process parameters on mechanical properties and their optimal selection." Materials & Design 124 (2017): 143-157.

[5] Ahn, Sung-Hoon, et al. "Anisotropic material properties of fused deposition modeling ABS." *Rapid prototyping journal* 8.4 (2002): 248-257.

[6] Casavola, Caterina, et al. "Orthotropic mechanical properties of fused deposition modelling parts described by classical laminate theory." *Materials & design* 90 (2016): 453-458.

[7] Kuznetsov, Vladimir, et al. "Strength of PLA components fabricated with fused deposition technology using a desktop 3D printer as a function of geometrical parameters of the process." *Polymers* 10.3 (2018): 313.

[8] Torres, Jonathan, et al. "Mechanical property optimization of FDM PLA in shear with multiple objectives." *Jom* 67.5 (2015): 1183-1193.

[9] Akhoundi, B., and A. H. Behravesh. "Effect of filling pattern on the tensile and flexural mechanical properties of FDM 3D printed products." *Experimental Mechanics* (2019): 1-15.

[10] Wittbrodt, Ben, and Joshua M. Pearce. "The effects of PLA color on material properties of 3-D printed components." *Additive Manufacturing* 8 (2015): 110-116.

[11] Kim, Eunseob, Yong-Jun Shin, and Sung-Hoon Ahn. "The effects of moisture and temperature on the mechanical properties of additive manufacturing components: fused deposition modeling." *Rapid Prototyping Journal* 22.6 (2016): 887-894.

[12] Ward, Ian M., and John Sweeney. *Mechanical properties of solid polymers*. John Wiley & Sons, 2012.

[13] Jones, David RH, and Michael F. Ashby. *Engineering materials 2: an introduction to microstructures, processing and design*. Elsevier, 2005.

[14] Grellmann, Wolfgang. Polymer testing. Ed. Sabine Seidler. Munich: Hanser, 2007.

[15] Van Melick, H. G. H., et al. "The influence of intrinsic strain softening on the macroscopic deformation behaviour of amorphous polymers." *Proceedings of the 15th annual meeting of Polymer Processing Society,'s-Hertogenbosch, The Netherlands' p10*. 1999.

[16] Engels, Tom AP, et al. "Time-dependent failure of amorphous polylactides in static loading conditions." *Journal of Materials Science: Materials in Medicine* 21.1 (2010): 89-97.

[17] Bergstroem, Joergen S., and Danika Hayman. "An overview of mechanical properties and material modeling of polylactide (PLA) for medical applications." *Annals of biomedical engineering* 44.2 (2016): 330-340.

[18] Tanikella, Nagendra G., Ben Wittbrodt, and Joshua M. Pearce. "Tensile strength of commercial polymer materials for fused filament fabrication 3D printing." *Additive Manufacturing* 15 (2017): 40-47